

Critic: a new program for the topological analysis of solid-state electron densities

A. Otero-de-la-Roza^{*}, M. A. Blanco,
A. Martín Pendás, and Víctor Luaña

Departamento de Química Física y Analítica, Facultad de Química, Universidad de Oviedo, 33006 Oviedo, Spain

Abstract

In this paper we introduce CRITIC, a new program for the topological analysis of the electron densities of crystalline solids. Two different versions of the code are provided, one adapted to the LAPW (Linear Augmented Plane Wave) density calculated by the WIEN2K package and the other to the *ab initio* Perturbed Ion (*aiPI*) density calculated with the PI7 code. Using the converged ground state densities, CRITIC can locate their critical points, determine atomic basins and integrate properties within them, and generate several graphical representations which include topological atomic basins and primary bundles, contour maps of ρ and $\nabla^2\rho$, vector maps of $\nabla\rho$, chemical graphs, etc.

PACS: 31.15.ae.

Key words: Quantum Theory of Atoms in Molecules (QTAIM), topological analysis, electron density, WIEN2K, *aiPI*.

PROGRAM SUMMARY

Manuscript Title: Critic: a new program for the topological analysis of solid-state electron densities.

Authors: Alberto Otero-de-la-Roza, M. A. Blanco, A. Martín Pendás, and Víctor Luaña.

Program Title: CRITIC

Journal Reference:

Catalogue identifier:

Licensing provisions: GPL, version 3.

Programming language: Fortran 77 and 90.

^{*} Corresponding author

Email address: alberto@carbono.quimica.uniovi.es (A. Otero-de-la-Roza).

Size: 46703 independent lines.

Operating system: Unix, GNU/Linux.

Number of processors used: 1.

Supplementary material: User's guide, test cases including input and output.

Keywords: Quantum Theory of Atoms in Molecules (QTAIM), topological analysis, electron density, WIEN2K, *aiPI*.

PACS: 31.15.ae.

Classification: 7.3 Electronic Structure

Nature of problem: Topological analysis of the electron density in periodic solids.

Solution method: The automatic localization of the electron density critical points is based on a recursive partitioning of the Wigner-Seitz cell into tetrahedra followed by a Newton search from significant points on each tetrahedra. Plotting of and integration on the atomic basins is currently based on a new implementation of Keith's promega algorithm.

Running time: Variable, depending on the task. From seconds to a few minutes for the localization of critical points. Hours to days for the determination of the atomic basins shape and properties. Times correspond to a typical 2007 PC.

LONG WRITE-UP

1 Introduction

Since its origins in the 1970 decade, the Quantum Theory of Atoms in Molecules (QTAIM) proposed by Bader et al. [1,2] has evolved to be an invaluable tool for the chemical interpretation of quantum mechanical data. The theory is built upon quantum mechanical observable quantities, like the electron density. Even though any practical implementation must rely on approximately obtained electron densities, QTAIM results are, in fact, quite independent from any basis set description of the density, an invaluable property for solid state studies, where a large variety of representations is used.

Conventionally, QTAIM starts from a particular division of real space into atomic basins, each containing a single maximum of the electron density, usually corresponding to a nucleus. Two neighbor basins are separated by an interatomic surface (IAS) such that the local flux of the electron density gradient is zero at every point of the surface. This condition provides the only partition that allows a unique definition of momentum based operators (like the kinetic energy operator) in a non-trivial subset of the real space. Given the appropriate operator density, any quantum mechanical observable can be integrated within the atomic basins, giving rise to the partition of properties into additive atomic contributions [3]. Charge and volume [4,5], but also multipolar momenta [6], polarizabilities [7], stress [8], magnetic susceptibility [9], or total energy [10,11] have been shown to be partitioned in this way.

QTAIM has been applied traditionally to molecular systems, so most of the previously existing software is not adequate for an infinite periodic density. CRITIC has intended, from its original versions [12], to fill this gap by providing a tool tailored for the analysis of densities of solids under the Born-von Karman conditions. The infinite and periodic nature of the problem confers particular features to the topological analysis:

- The atomic basins are bounded in \mathbb{R}^3 . The zero-flux surfaces never stretch infinitely away from the nucleus.
- The number of critical points (CPs) in the unit cell fulfills the Morse relationships:

$$n - b + r - c = 0, \quad n, c \geq 1, \quad b, r \geq 3, \quad (1)$$

where n is the number of local maxima, usually called nuclear critical points (ncp); b , bond critical points (bcp); r , ring critical points (rcp) and c , the number of cage critical points (ccp). The first Morse relationship is analogous to the Euler-Poincaré equation which applies in finite systems, for

which the asymptotic minimum at the infinite has been removed. The ring and cage points, compulsory in solids, are uncommon in small molecules.

- The crystal symmetry forces the existence of CPs at selected positions in the unit cell. Specifically, every fixed Wyckoff position forcibly contains at least a CP. Also, the unit cell may be partitioned by the action of the symmetry operations. The smallest wedge of the Wigner-Seitz cell that holds all the motif information (the irreducible wedge of the Wigner-Seitz cell, IWS) also contains one and only one copy of each non-equivalent CP.
- Atomic basins, defined as the geometric locus of all electron density gradient field lines attracted to a given nuclear critical point, are neither the only nor the minimal partition compatible with the zero flux condition.
- Bounded primary bundles[12] may be defined. A primary bundle is formed by the set of points which share α - and ω -limit, i.e. start and end points for the electron density gradient descent paths. Atomic basins are formed by the union of all primary bundles sharing the same α -limit, i.e. the same ncp. Similarly, the repulsion basins of the electron density local minima (voids in the crystal structure) can be defined as the union of the primary bundles that share the same ω -limit, i.e. the same ccp.

QTAIM analysis is essentially based on two main tasks. The first one is computationally cheap, when done efficiently, and involves the localization of the critical points of the electron density and the characterization of their properties. The bcp properties facilitate the classification of the crystal into shared-shell (i.e. covalent) and closed-shell systems. The chemical graph can also be drawn from the knowledge of all CP's. The second task, computationally more involved, corresponds to the determination of the primary bundles or the atomic basins and the integration of quantum mechanical properties within them. The complexity of this second step is due to the non-local nature of the zero-flux condition,

$$\nabla\rho(\mathbf{r}) \cdot \mathbf{n}(\mathbf{r}) = 0, \tag{2}$$

which holds for every point \mathbf{r} on the atomic basin separatrix. This zero-flux surface is, in practice, quite difficult to find. Several algorithms have been tried [13–20] but to date only the low-efficient bisection algorithm has proven reliable enough on crystals.¹ Atomic basins may adopt quite complicated geometries on crystals, some of them presenting thin wings and needles [22] to accomodate the rcp and ccp that form the edges and vertices of the IAS's. The gradient lines that form the zero-flux surface itself tend to be strongly directed towards some of the attracting critical points, leaving other attractors almost empty of gradient lines [23]. Basin integration needs to surpass these difficulties to produce a good sampling of the basin volume.

We have developed the CRITIC program with the goal to be a general pur-

¹ Notice, however, the promising finite elements technique recently developed by Rafat and Popelier [21] for molecules.

pose solid state topological analysis utility. The code interprets the density files obtained from different electronic structure programs and serves as a platform to develop new integration algorithms. In this first public version, CRITIC accepts two different types of electron densities: those obtained in a full-potential linearized augmented plane-waves(FPLAPW) calculation [24,25] using the WIEN2K package [26,27]; and those calculated using the *ab initio* perturbed ion (*ai*PI) formalism [28,29], as implemented in the PI7 program [30]. Promolecular densities can be treated as a particular case of *ai*PI. CRITIC is able to perform all the basic topological tasks, which include determining topological quantities in points, lines, planes and three-dimensional sets, automatically locating the CPs of the electron density, integrating atomic properties, and generating representations of atomic basins, primary bundles, gradient paths and contour and relief plots of ρ and $\nabla^2\rho$.

In the rest of the paper we present a glimpse of the theory behind both the FPLAPW and the *ai*PI methods (Section 2) and we describe the CRITIC program (Section 3).

2 The FPLAPW and the *ai*PI methods

The FPLAPW method is based on the Kohn-Sham formulation of the density functional theory (DFT)[31,32]. It is one of the most accurate electronic structure methods available, owing to the fact that no approximation is made to the crystal potential near the nuclei. The real space is split in two regions: spheres centered on the nuclei (*muffin tin* region, S_α) and the interstitial region (I). Each one electron basis function is then made of an atomic-like spherical harmonics expansion within the muffin and a single plane wave in the interstitial:

$$\phi_{\mathbf{K}}^{\mathbf{k}}(\mathbf{r}) = \begin{cases} \frac{1}{\sqrt{V}} e^{i(\mathbf{k}+\mathbf{K})\cdot\mathbf{r}}, & \mathbf{r} \in I, \\ \sum_{lm} [A_{lm}^{\alpha,\mathbf{k}+\mathbf{K}} u_l^\alpha(r', E_{1,l}^\alpha) + B_{lm}^{\alpha,\mathbf{k}+\mathbf{K}} \dot{u}_l^\alpha(r', E_{1,l}^\alpha)] Y_l^m(\hat{r}'), & \mathbf{r} \in S_\alpha, \end{cases} \quad (3)$$

where V is the cell volume; \mathbf{k} is a vector in reciprocal space; \mathbf{K} is a reciprocal lattice vector; \mathbf{r}' is the real space position relative to the atom α and \hat{r}' its angular coordinates; and Y_l^m is a spherical harmonic function. The atomic radial part, u_l^α , and its radial derivative, \dot{u}_l^α , are obtained by solving an effective central-field problem for atom α with the enforced linearization energy $E_{1,l}^\alpha$, typically a Dirac-Fock relativistic equation. The coefficients $A_{lm}^{\alpha,\mathbf{k}+\mathbf{K}}$ and $B_{lm}^{\alpha,\mathbf{k}+\mathbf{K}}$ are determined by trying that the two parts of $\phi_{\mathbf{K}}^{\mathbf{k}}(\mathbf{r})$ match in value and slope on the *muffin* surface. The match could only be perfect in the limit of an infinite expansion in spherical harmonics.

From our point of view, the advantage of the FPLAPW method is that no pseudopotential is used. Therefore, the total electron density is directly available for the QTAIM analysis. In fact, since a relativistic Dirac-Fock calculation is used to determine the intra muffin density, and a scalar relativistic approach is applied to the interstitial region, the FPLAPW calculations should be expected to work excellently, and consistently, from light to heavy nuclei crystals.

The electron density in the FPLAPW scheme is given by an analytical expression analogous to that of the basis functions:

$$\rho(\mathbf{r}) = \begin{cases} \sum_{LM} \rho_{LM}(r') Y_L^M(\hat{r}'), & \mathbf{r} \in S_\alpha, \\ \sum_{\mathbf{K}} \rho_{\mathbf{K}} e^{i\mathbf{K}\cdot\mathbf{r}}, & \mathbf{r} \in I. \end{cases} \quad (4)$$

The density in the muffin tin region is given by a multipolar expansion, i.e. a sum of spherical harmonics with radial coefficients $\rho_{LM}(r')$. The expression changes in the interstitial region to a Fourier expansion, with \mathbf{K} representing a reciprocal lattice vector. The continuity of the electron density at the muffin border can only be guaranteed by using an infinite number of spherical harmonics within the muffin, but the discontinuities are usually small and can be neglected in most cases.

CRITIC also works with electron densities obtained via the *ai*PI method. This formalism is based on an extension of the Theory of Electronic Separability by McWeeny and Huzinaga[33–35,28]. Each atom is regarded as a group that interacts weakly with the rest of the atoms in the crystal. The group wave function is approximated by the antisymmetrized product of atomic orbitals, self-consistently calculated as linear combination of atomic basis functions (usually STOs) in a way similar to an atomic Hartree-Fock calculation, but including the classical and quantum effects of the rest of the groups in the external potential. An iterative process is carried out where the group wave functions are optimized one at a time, under the updated potential of the crystal, until the whole set is consistent. The total wave function is the antisymmetrized product of the group wave functions.

The *ai*PI method is an excellent choice for ionic (closed-shell) systems, being both fast (it scales linearly with the size of the system [36]) and reliable. However, the requirement for weak interaction among groups limits its applicability to other compounds.

The electron density in the *ai*PI method is calculated as a sum over group contributions:

$$\rho(\mathbf{r}) = \sum_S \rho_S(\mathbf{r}) \quad (5)$$

where the sum runs over all the atoms in the crystal. The group densities are

generated adding up the atomic orbital contributions:

$$\rho_S(\mathbf{r}) = \sum_{nl} n_{nl}^S \sum_{pq} c_{nlp}^S c_{nlq}^S \chi_{pl}^S(r) \chi_{ql}^S(r) \quad (6)$$

where n_{nl} is the number of electrons in the n, l subshell, χ_{pl} are the basis functions (STOs) and c_{nlp} are the coefficients for the atomic orbital linear combination. Note the spherical symmetry of the group electron densities. The promolecular (or procrystal) electron densities can be treated as if they were *aiPI* ones.

3 Description of the program

3.1 Capabilities and algorithms

CRITIC provides the capabilities expected from a fully-fledged topological analysis program. These include:

- Determination of electron density properties ($\rho, \nabla^2\rho, \dots$) on arbitrary points in the unit cell.
- Integration of gradient paths passing through arbitrary points.
- Automatic localization of all CPs and, optionally, checking a user-entered collection of points for their CP character.
- Determination of atomic basins and primary bundles. Several plot representations of those objects are available using external graphing programs.
- Integration of topological properties on atomic basins. As of this version, these properties include volume and charge for the WIEN2K flavour of CRITIC. In the *aiPI* version, also force, stress[8] and kinetic energy are computed.
- Contour representations of ρ and $\nabla^2\rho$ in a selected plane.
- One, two and three-dimensional plots of $\rho, \nabla\rho, |\nabla\rho|$, and $\nabla^2\rho$.
- Representation of gradient paths, either projected on a plane or in a three-dimensional display.
- Zero-flux surface plots, including atomic basin separatrices and primary bundles. Also, CRITIC can generate plots of isosurfaces of density inside an atomic basin.

Two main tasks lie at the core of the topological code and the algorithms used deserve an adequate description. First, CRITIC makes full use of the crystal symmetry to build the irreducible wedge of the Wigner-Seitz (IWS) cell. The IWS, formed by one or more tetrahedra, is recursively subdivided up to a specified level by placing new points at the center of the edges, faces and the interior of each tetrahedra. The localization of CPs is then carried out

by means of a Newton-Raphson (NR) search starting from each corner, edge, face, and interior of the above partition. When the search process has finished, the list of CP candidates is completed and pruned by applying the symmetry operations and removing duplications. This approach provides a considerable improvement over the traditional search over doubles, triplets and quartets of atoms, specially in highly symmetric crystals. Even more important, the search based on the IWS guarantees that every Wyckoff position is visited at least once thus facilitating the localization of some elusive rcp and ccp showing a very small NR capture basin. The result is a quite robust algorithm that automatically locates all CPs, including the non nuclear maxima exhibited by some crystals [37,38].

The topological task is completed by determining, for each type of bcp and rcp, the *bond path* that connects a bcp with its two neighbor maximal attractors (usually ncp's), and the similar path connecting each rcp to its minimal repellers (usually ccp's). A depiction of the bond paths produces the chemical graph of the system. Adding the ccp-to-rcp paths commonly results in a molecular graph of excessive complexity to be useful and, even so, the complete topological graph still needs a further type of lines: bcp's and rcp's are connected by single gradient paths which correspond to the intersection between the IAS generated by the bcp and the analogous ring surface. Determining those bcp-to-rcp lines is quite difficult, in practice.

The second main task worth noticing is the determination of the atomic basins and the integration of the basin additive properties. The method used by CRITIC is currently based on the promega algorithm developed by T. Keith [13]. The algorithm works by determining the limit of the basin for a collection of rays emanated from the basin inner attractor. Any point along the ray belongs in the basin if the upwards gradient path traced from this point flows into the basin attractor, and it belongs in a different basin otherwise. The surface position is initially bracketed by a point quite close to the attractor and a point sufficiently far from it. The bracket is refined using a binary partition scheme until some convergence threshold is achieved. The whole process is slow and dominated by the time used to trace the gradient path from each test point. However, the convergence to the real zero-flux surface is assured to the required precision. A possible glitch on this scheme is the scenario in which a ray intersects the separatrix more than once. However, we have never observed this multiple intersection behavior in solids and only on rare occasions in molecules.

The selection of rays depends on the task at hand. For the purpose of depicting the basin we prefer to use a tessellation of the sphere based on a regular polyhedron, typically a cube or octahedron, whose surface is recursively divided to achieve some 1000–6000 rays, depending on the resolution desired for the plot. When integrating, the limit of the atomic basin is determined along the

rays whose angles correspond to the nodes of Gauss-Legendre quadratures in spherical coordinates.

With small changes the above method can also be used to trace primary bundles. In this case we must require that both, the α - and the ω -limits of each trajectory, correspond to those of the bundle currently being examined. An additional difficulty is the selection of a point inside the bundle as the origin of the rays. Whereas the ncp is the natural origin for an atomic basin, no critical point occurs inside a primary bundle. The bundle surface, on the other hand, contains one ncp and one ccp (forming the north and south poles of the bundle), and an equal number of bcp and rcp (forming the bundle equator). Three reasonable selections for the origin are: the midpoint between the poles, the baricenter of the equator points, and the baricenter of all the CPs. In any case, neither candidate is guaranteed to be interior to the desired bundle.

3.2 *Input description*

CRITIC reads an input file which contains the structural and electronic information for the system and the orders to execute. As a detailed description of the available keywords would be too long, we present here only a selection of the most relevant ones and refer the reader to the user's guide, distributed with the code, for further detail. During the following discussion, verbatim keywords are written in **CAPITALS** to distinguish them from variables, in **smallcase**. The type of each variable is indicated by a suffix: **.s** for a string, **.i** for an integer and **.r** for a real value. Also, square brackets indicate an optional argument and curly braces with vertical bars, alternative keywords. When a complete order exceeds the space available for a line of text, the continuation is shown strongly indented in the next line or lines. The selected orders are:

- **CRYSTAL**: the crystal environment is usually the first specification in a CRITIC run as it provides the information about the system. Its form depends on whether the WIEN2K or the *ai*PI version of CRITIC is being used. In the case of the WIEN2K version, everything can be read from two WIEN2K files: the **.struct** file, containing the crystal structural data, and the **.clmsum** file, holding the electron density expansion coefficients. Henceforth, a CRITIC input should start with

```
CRYSTAL
  STRUCT structfile.s
  CLM clmfile.s
  [CLMDOWN clmdown_file.s]
ENDCRYSTAL
```

where the **CLMDOWN** order is used on spin-polarized calculations, on which

two different `.clm` files describe the spin-up and spin-down electron density.

The `aiPI` version, on the other hand, requires the user to enter explicitly the crystallographic description of the crystal:

```
CRYSTAL
  SPG spg.s
  CELL a.r b.r c.r alpha.r beta.r gamma.r
  NEQ x.r y.r z.r atomfile.s
ENDCRYSTAL
```

The `spg.s` string is expected to contain a list of the independent elements that form the space group description. For instance, $Fm\bar{3}m$ should be entered as "f m -3 m", $P6_3/mmc$ as "p 63/m m c", and $R32$ as either "r 3 2" (default hexagonal axes) or "r 3 2 r" (rhombohedral axes). Cell lengths (in bohr) and angles (in degrees) define the unit cell. The crystal description is completed by entering a `neq` order for every nonequivalent atom in the unit cell. This order gives the crystallographic coordinates (x, y, z) and the name of the `PI7` atom file containing the local group wavefunction [39,30].

- **AUTO:** This deceptively simple order activates the complex task of completing the topological characterization of the crystal CPs. The recursive division depth of the irreducible Wigner-Seitz zone (IWS) can be increased beyond the default value of 2, which might prove to be necessary if the unit cell contains a huge number of atoms and thus of CPs. The user can also request to start from a partition of the whole parallelepipedic cell instead of from the IWS, but this is not recommended in general. Several searching methods are available, but the default Newton-Raphson is the best in nearly all cases. The order can be completed, optionally, with the gradient norm threshold, used to accept or reject the CP candidates, and the absolute and relative limits for a density change between steps:

```
[SET [NO]IWS [depth.i]]
  AUTO {NEWTON|AMOEBA|...} [gradthr.r [abstol.r [ftol.r]]]
```

- **INTEGRALS:** integrate the atomic properties in the atomic basins. The default is to run over all the nonequivalent atomic basins known to the code. This would include possible non nuclear maxima in the case that a previous `auto` search has found them. Running `auto` before `integrals` is thus advisable and adds almost nothing to the integration time. The complete syntax for the order is

```
INTEGRALS [thetai.r thetalf.r phii.r phif.r]
  nr.i ntheta.i nphi.i
  [NCP id.i]
```

where `thetai.r ... phif.r` are the initial and final values of the angular coordinates θ and ϕ for the integrals. The default is $(0, \pi, 0, 2\pi)$ corresponding to the whole basin for each atom. The (n_r, n_θ, n_ϕ) (`nr.i, ...`) values correspond to the number of nodes used on the spherical quadrature: n_θ and n_ϕ determine the number of rays and n_r the number of points along each ray. The `NCP` option, finally, is used to restrict the integration to the basin of a single `nep`.

The local symmetry around a ncp can be used to reduce the region of integration. A wedge made of one third of the basin would be enough, for instance, if a \hat{C}_3 axis passes through the ncp. CRITIC is smart enough to determine the multiplication factor that converts the wedge integral to the whole basin one, but it does not determine nor checks the integration wedge entered by the user. This is intended to change in future versions of the code.

- **DOPLOT**: this keyword is used to create one, two and three-dimensional representations of ρ , $\nabla^2\rho$, $\nabla\rho$ and $|\nabla\rho|$ in a variety of formats. The syntax is:

```
DOPLOT [DENSITY | LAPLACIAN | ...]
       [FORMAT [GNU PLOT | CUBE | ...]]
       [FILE root.s]
       { 1D  x0.r y0.r z0.r  x1.r y1.r z1.r  npts.i
         | 2D  x0.r y0.r z0.r  x1.r y1.r z1.r
           x2.r y2.r z2.r  n1.i n2.i
         | 3DC x0.r y0.r z0.r  x1.r y1.r z1.r
           n1.i n2.i n3.i }
```

Several output formats are available, depending on the requested plotting task. In the case of the 1D plot, for instance, the GNU PLOT [40] output is the most convenient, as it includes a large number of properties evaluated on the $\mathbf{r}_1 - \mathbf{r}_0$ segment. In the case of the 2D and 3D plots, however, only one property is available at each time, with the electron density being the default. Nothing prevents, however, producing several data files from successive `doplot` orders, and combining them with the appropriate drawing software.

The 2D plane is determined from the crystallographic coordinates of three points: \mathbf{r}_0 , \mathbf{r}_1 , and \mathbf{r}_2 . The $\mathbf{r}_1 - \mathbf{r}_0$ segment is the abscissa, and $\mathbf{r}_2 - \mathbf{r}_0$ the ordinate of the plot. In the case of a 3D plot, the gridded volume is defined by the two extreme points along the main diagonal of a parallelepiped, plus the number of points to use on each direction.

Figure 1 contains an example of a 3D `doplot` representation. The depiction of successively increasing or decreasing isosurfaces can be used to identify maxima and minima of a scalar field and the existence of paths connecting these peaks and pits. Short of a true critical point determination, this technique can be used to investigate the topological properties of, say, $\nabla^2\rho$. The `cube` format can be exported to codes like MOLEKEL [41] and TESSEL [42] to help in this task.

- **GRDVEC**: Given a user defined plane, this versatile order plots the gradient paths starting at arbitrary points within the plane, optionally combined with contour maps of the electron density or laplacian. The main orders within this section are:

```
GRDVEC
      FILES rootname.s
      PLANE x0.r y0.r z0.r x1.r y1.r z1.r x2.r y2.r z2.r
      [ORIG x.r y.r z.r atr.i up.i down.i]
```

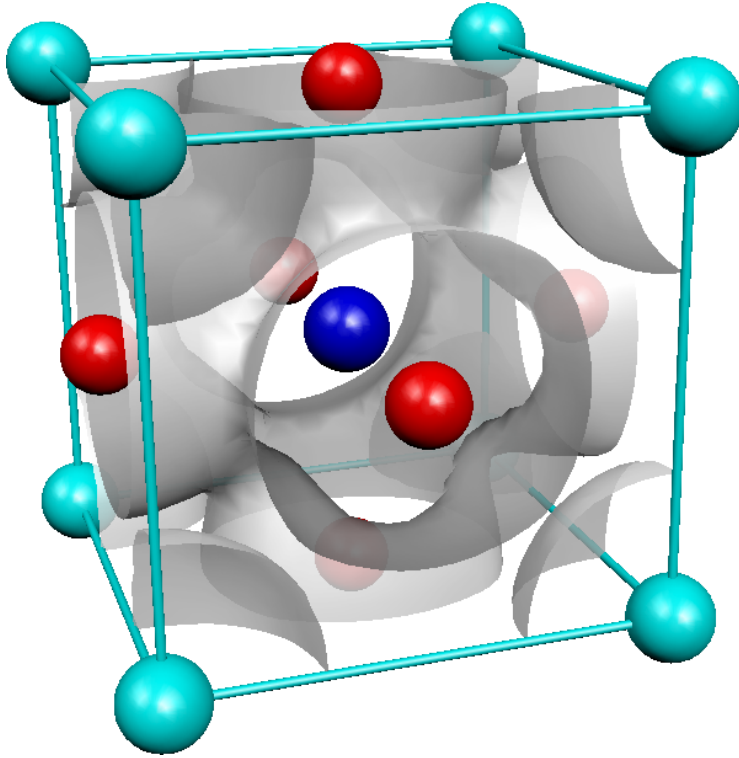


Fig. 1. 0.02 e/bohr^3 electron density surface of the CaTiO_3 perovskite unit cell produced with the `doplot/3dc` order and rendered with `TESSEL` [42] and `POVRAY` [43].

```
[CP id.i up.i down.i]
[CPALL]
[BCPALL up.i down.i]
[CHECK
  x.r y.r z.r
  ...
ENDCHECK]
[{RHO|LAP|...} [LOG|ATAN|...] [nu.i [nv.i [niso.i]]]]]
ENDGRDVEC
```

Three points (\mathbf{r}_0, \dots), given in crystallographic coordinates, determine the plane of the plot: \mathbf{r}_1 serves as the origin, $\mathbf{r}_1 - \mathbf{r}_0$ is the abscissa (u axis) and $\mathbf{r}_2 - \mathbf{r}_0$ the ordinate (v axis). The points that form part of the plot are automatically converted to orthogonal in-plane coordinates to prevent distortion in non-orthogonal crystalline systems or, simply, if the abscissa and ordinate are not perpendicular.

The source points for the gradient vector lines can be entered in several ways. With the `orig` and `cp` orders the user selects an arbitrary location (x, y, z) or a specific critical point (the label number from a previous `auto` order), respectively. The user must indicate the number of trajectories going up and down and, in the case of the `orig` order, the `atr` value marks whether this point corresponds to a nucleus or not.

The `cpall` and `bcpall` orders are smarter: the CPs are replicated by symmetry and the program selects all the CPs (or just the bcp's) which actually lie in the plane. This decision only works if an `auto` order has been done before `grdvec`. Alternatively, the user can provide, within a `check` environment, a list of potential targets, that will be replicated by symmetry and used only if they truly are critical points and belong to the plane.

The plot can include, optionally, a contour representation of the electron density or its laplacian. The electron density map is dominated by the large peaks at the nuclei, roughly proportional to the cube power of the nuclear charge, but the most important information from a chemical point of view lies in the valence region, with a density of some 10^{-1} – 10^{-3} e/bohr³, orders of magnitude smaller than the nuclear peaks. A logarithmic scale on the contour levels (`log` option in the `rho` order) helps in visualizing the valence part, with negligible distortion, while keeping the nuclear densities in the plot. We can observe the result of a typical density plus gradient field lines in Fig. 2a.

Similarly, the electron density laplacian varies from $-\infty$ to $+\infty$, but the chemical information lies in the positive and negative values close to zero. A scale based on the arc tangent function, $(2/\pi) \tan^{-1}(\nabla^2\rho)$ (the `atan` option in the `lap` order), provides a convenient way to visualize the laplacian in the valence region. Negative and positive laplacian zones map the electron rich and electron poor regions. Besides the atomic like shell structure exhibited around the nuclei, a bcp lying in a negative zone is a clear sign of covalent bonding. This is quite evident on the graphene sheets depicted in Fig. 2b. The graphite structure shows two different C-C bcp's: the covalent short range bond shown in the graphene plane, and the much weaker, closed-shell like, bcp that links together two planes. The difference between both bcp's is quite evident in the b and c parts of Fig 2.

- **fluxprint**: this started as a simple internal task used to debug the gradient vector field routines. Accordingly, the first order was quite simple:

```
FLUXPRINT POINT {1|-1|0} x.r y.r z.r [step.r [epsi.r]]
```

asking the code to trace the $\nabla\rho(\mathbf{r})$ line that passes through the (x, y, z) point (in crystal coordinates) and goes up (+1), down (-1), or both ways (0). The trajectory is integrated using an adaptive Euler method that begins with the indicated `step` value (0.1 as a default) and continues until the absolute value of the gradient falls below the `epsi` threshold (10^{-7} as a default). Other integration techniques have been implemented, but the adaptive Euler method has proven to be both robust and fast.

More advanced tasks have been added to `fluxprint`. For instance

```
FLUXPRINT NCP id.i ntheta.i nphi.i [step.r [epsi.r]]
[LVEC x.i y.i z.i]
```

is used to trace a star of field lines around the `id`-th NCP (according to the complete list of CPs in the unit cell written by a previous `auto` task). The number of field lines is determined by a linear grid in the polar spherical angles θ and ϕ . The optional `lvec` parameter adds an integer displacement

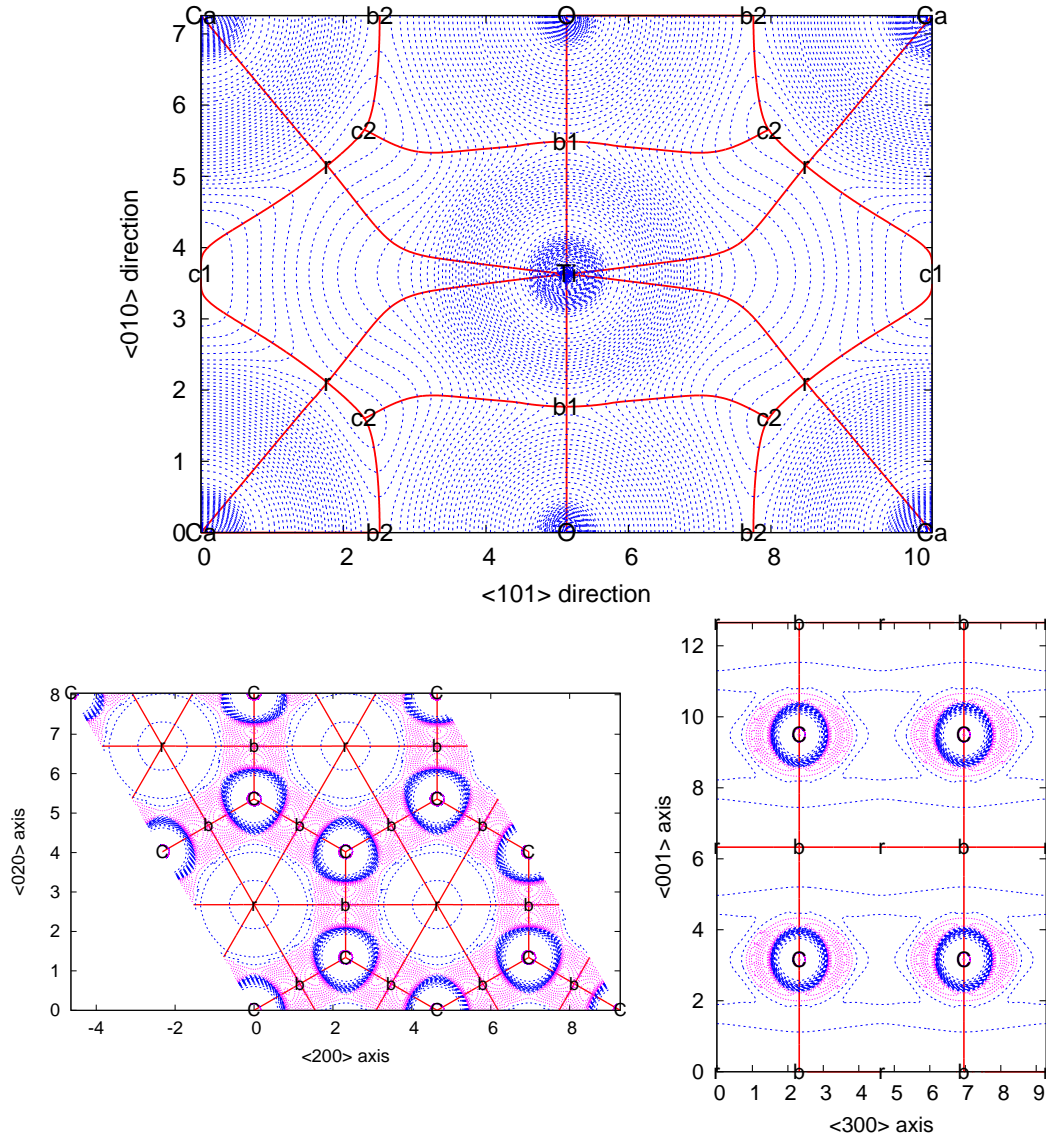


Fig. 2. (Top) Electron density of CaTiO_3 in the $[\bar{1}01]/\sqrt{2}$ plane. This plane contains all the CPs of the structure: the three nuclei, the Ca-O and Ti-O bcp's, a single rcp, and two different ccp's. Being also a symmetry plane of the structure, the down trajectories from the bcp's and the up trajectories from the rcp show the limits of the central Ti basin, including the characteristic wings that will be clearly depicted in Fig. 4.

(Bottom) Electron density laplacian of graphite on a graphene plane (left, $[001]$) and on a perpendicular plane (right, $[\bar{1}, \sqrt{3}, 0]/2$). The C basin is, essentially, a triangular prism. The hexagonal arrangement of C atoms around a ring CP is a quite typical feature of this structure.

Thick red lines correspond to $\nabla\rho$ trajectories, blue (magenta) lines are positive (negative) contours of ρ (top) and $\nabla^2\rho$ (bottom).

vector to the origin coordinates, thus allowing the user to start from a different unit cell.

Similar orders exist to trace field lines that start on any bcp, rcp, or ccp within the crystal.

The most complex `fluxprint` order is, currently

```
FLUXPRINT GRAPH igrph.i [step.r [epsi.r]]
```

intended to trace the complete chemical graph, i.e., the minimal set of paths that connects all CPs in the main cell, including the portion of the paths to the CPs in neighbor cells that lie inside the main one. The graph is made of a variety of lines, that the user can select by type, switching on and off the corresponding bits in the `igrph` control integer:

- bit 1: ring paths, i.e. the unique two single paths that flow downwards from each rcp to their ccp sinks. Use `igrph=1` to ask only for these lines.
- bit 2: bond paths, i.e. the unique pair of paths flowing upwards from each bcp to their ncp sources. These are the only paths produced if `igrph=2` (i.e. binary 0010).
- bit 3: the *stable paths* on the interatomic (IAS) and on the ring surfaces. In the case of IAS the connection between the central bcp and each ccps lying on the IAS border forms a 2D stable domain. On the contrary, the connection between the central bcp and each rcp, also lying on the IAS border, forms a 1D unstable domain, quite difficult to determine. A minimal length trajectory can be used to represent each 2D bcp-to-ccp stable domain, although `fluxprint/graph` simplyfies right now the task by depicting a single rectilinear stick between the bcp and the ccp positions. The same concept applies to the ring surfaces, but now a single rcp is the origin of the surface, rcp-to-ncp 2D bundles form the stable domains, and rcp-to-bcp 1D domains are the unstable class. The representation of the stable paths depends on some expensive data that the `auto` task will obtain only if the `set graph` option is explicitly activated.
- bit 4: the *unstable paths* just described, i.e. the bcp-to-rcp trajectories. Notice that every bcp-to-rcp path corresponds to the intersection between the IAS generated by the bcp and the ring surface created by the rcp. Except when determined by symmetry, those paths use to form a curved line quite difficult to find. Currently, this trajectory is represented by a single stick in the graph plot. The connectivity between bcp's and rcp's is only obtained is the `auto` task is carried with the `set graph` option before doing `fluxprint`.

The most useful graph is generally the one obtained with `igrph=2` and `igrph=15` produces the most complete connectivity graph.

Fig. 3 depicts a ncp, a bcp, and a graph image obtained on the γ -Fe (FCC, Face Centered Cubic) structure. The topology of this crystal shows a single type of bcp's and a single type of rcp's, both situated on symmetry planes of the unit cell. The Fe basin is thus identical to the Wigner-Seitz cell. The two types of ncp appear clearly different on the IAS plot: bcp-ccp trajectories accumulate heavily towards the ccp of lowest electron density.

The bcp shows a rather typical ellipticity: 3.45, corresponding to the ratio between the two negative eigen curvatures of the electron density.

- **basinplot**: Our last selected task is in charge of writing a three-dimensional model for the zero-flux surface associated to every non-equivalent ncp in the unit cell. This model is obtained by determining the intersection of the zero-flux surface with rays centered on the corresponding ncp. These rays are generated by recursive subdivision of a cube or a octahedron. As it requires the determination of the limit of the interatomic surface for a large number of points, **basinplot** is rather computationally intensive. The order syntax is

```
BASINPLOT [lv1.i [delta.r [phasetheta.r [phasephi.r]]]]
```

The subdivision level is determined by the absolute value of `lv1`. If this integer is greater than zero, an octahedron is chosen as the starting polyhedron while for `lv1` lower than zero, **CRITIC** uses a cube. The current default value is `lv1=-3`. The value `delta` specifies the precision with which the zero-flux surface is determined (default: 10^{-5}). Finally, in highly symmetric cases, a foul representation of the basins may occur when some rays are traced along symmetry elements. To prevent this, a small rotation, determined by the `phasetheta` and `phasephi` angles, can be applied to the initial cube or octahedron.

Modelled after this task, **bundleplot** can be used to determine the primary bundles, and **basindensity** samples a collection of electron density properties along the rays used to define the atomic basin.

Fig. 4 shows the atomic basins of the CaTiO_3 perovskite. The Ca basin is basically a rhombidodecahedron, with nearly flat faces and edges. The Ca-O bcp is a notorious feature in the color decoration of each face. The Ti basin is a cube in which each edge has been extended to form a nearly bidimensional wing. This conspicuous element of the Ti geometry prevents the occurrence of O-O bond paths. Starting from the topology of the cube, with 6 faces (Ti-O bcp's), 8 vertices (ccp's) and 12 edges (rcp's), every edge has been decoupled into a vertex and two edges, for a total of 6 faces, 24 edges and 20 vertices. Correspondingly, a square and four triangles form a single face in the O basin (the Ti-O IAS), which is formed of 4+2 faces (Ca-O and Ti-O bcp's, respectively), 12 vertices and 16 edges. The image of the three basin types glued together shows that every M -O IAS is curved in such a way that the M basin is convex and the O basin has the concavity. This is a general property related with the relative electronegativity of the cation-like and the anion-like elements [44].

3.3 Code distribution

The source code is provided in a single *tar+gzipped* file. Once unpacked, the next subdirectory tree is created:

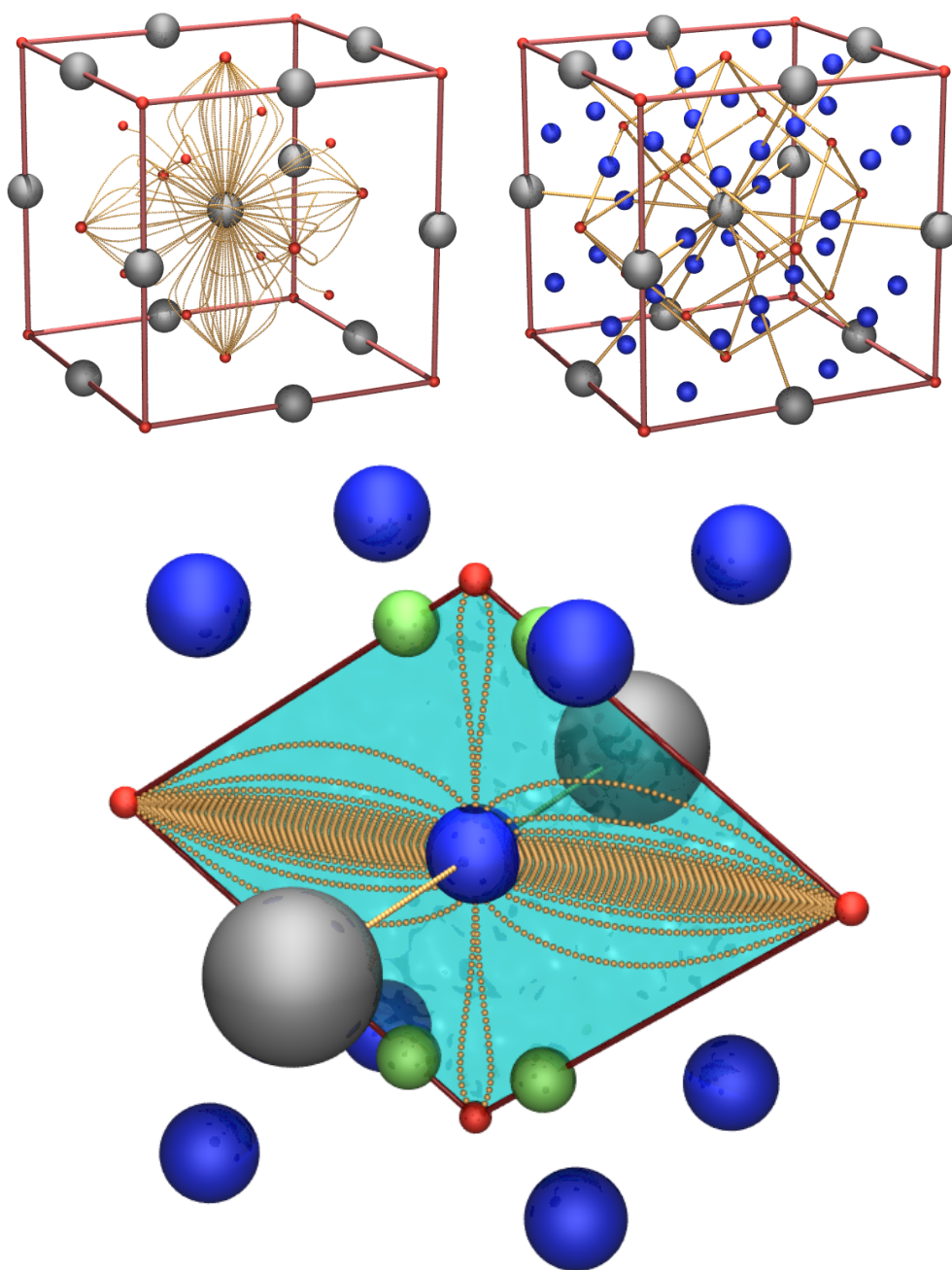


Fig. 3. Example of the fluxprint plots on the γ -Fe (FCC) structure. Grey, blue, green, and red balls of decreasing size are used to represent Fe atoms, bcp's, rcp's, and ccp's, respectively; a red frame marks the main cubic cell; and yellow curves show the gradient field trajectories. The top images correspond to the 3D attraction basin of a Fe atom (left) and to a `igraph=3` (bits 1 and 2) chemical graph (right) where rcp balls have been eliminated for simplicity. The bottom image shows the detail of a Fe-Fe IAS, obtained with a `fluxprint bcp` order. The accumulation of trajectories towards the acute rhombus vertices, in detriment of the obtuse vertices, is typical of most IAS.

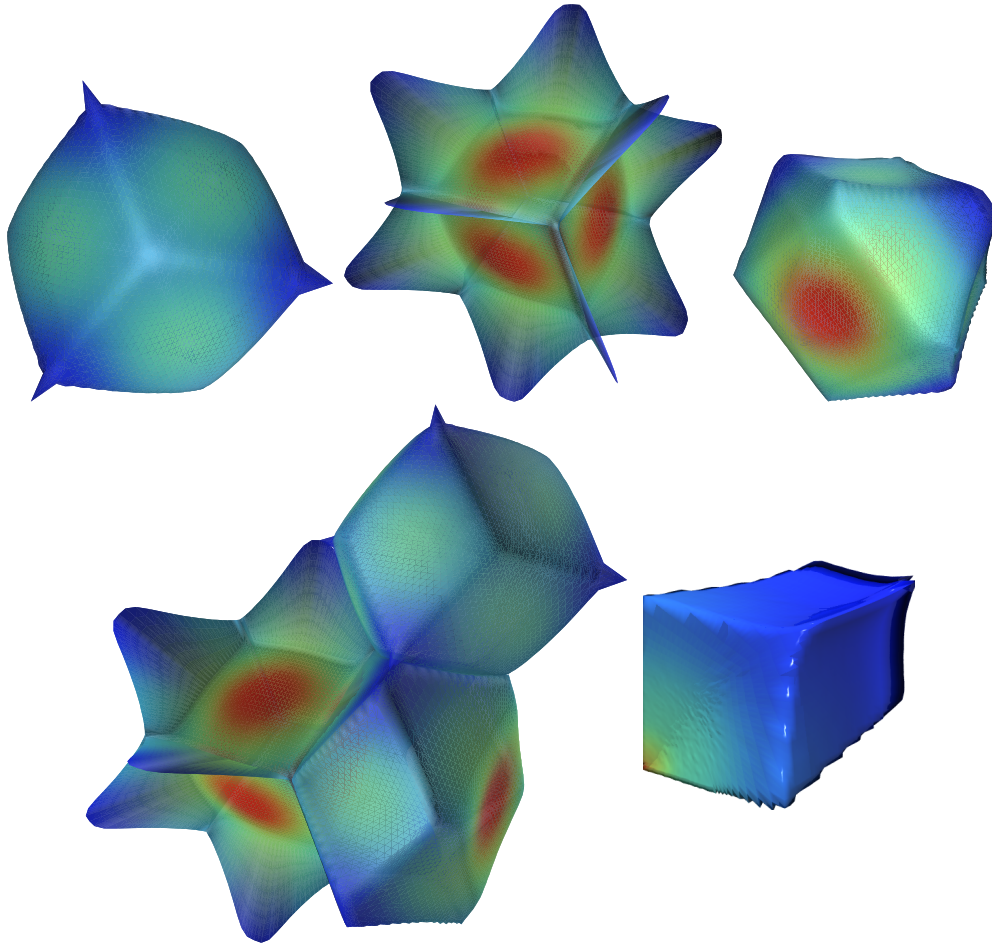


Fig. 4. Top: atomic basins for Ca (left), Ti (center) and O (right) in the CaTiO_3 perovskite. The color scale represents the logarithm of the electron density. Note the extremely thin wings in the Ti basin. Bottom: the three atomic basins connected together (left) and detail of a primary bundle of the Ti basin. The bundle algorithm, starting from the (0.56, 0.57, 0.58) point has not been able to detect the wings in this case.

- doc:** User guide written in a single ASCII file (`user-guide.txt`) with the `reStructuredText` markup [45]. A PDF and HTML version of the user guide can be automatically compiled from the ASCII document. Both are included in the distribution for simplicity.
- src:** Source code for the `WIEN` and `PI` versions of `critic`.
- tools:** Source code for a collection of programs useful when dealing with the `OFF`, `BASIN`, etc, geometric data files. A description of the data formats and the purpose and use of the tools is included in the user guide.
- test:** A collection of test cases to be used in checking the code performance and useful as templates for other crystals. The selected systems are: CaTiO_3 , Cu_3N , and the α - and γ -Fe structures.

A `README` file contains detailed instructions for the compilation on a unix-like environment. Basically, running `configure` and then `make` should compile all

executables: `criticw` and `criticp` (in `src/`), `off2off` (in `tools/off2off`), etc. Follow the instructions from the `INSTALL` file to move the executables to a general place accessible to all users. Alternatively, we advise to create a symbolic link to the executables in a user `/bin` directory and adding this directory to the user `PATH` variable.

On the other hand, `CRITIC` output is designed to interface with a set of programs freely available:

- `GNUPLOT`[40]: an open-source plotting program.
- `GEOMVIEW`[46]: an interface to view three dimensional geometric objects.
- `TESSEL`[42]: a program for the creation of high-quality three dimensional representations of crystal and molecular structures.
- `POVRAY`[43]: a raytracing renderer.

4 Acknowledgements

The development of this code has been done under financial support from the Spanish Ministerio de Educación y Ciencia and the ERDF of the European Union (project no. CTQ2006-02976). One of us (AOR) is indebted to the Spanish MEC for a FPU grant. The authors belong to the MALTA group (CSD2007-0045 project, MEC Consolider Ingenio 2010 program).

References

- [1] R. F. W. Bader, *Atoms in Molecules. A Quantum Theory*, Oxford University Press, Oxford, 1990.
- [2] R. F. W. Bader, A quantum-theory of molecular-structure and its applications, *Chem. Rev.* 91 (1991) 893–928.
- [3] R. F. W. Bader, P. L. A. Popelier, Atomic theorems, *Int. J. Quantum Chem.* 45 (1993) 189–207.
- [4] R. F. W. Bader, J. R. Cheeseman, C. Chang, M. T. Carroll, Properties of atoms in molecules. Atomic volumes, *J. Am. Chem. Soc.* 109 (1987) 7968–7979.
- [5] R. F. W. Bader, P. F. Zou, An atomic population as the expectation value of a quantum observable, *Chem. Phys. Lett.* 191 (1992) 54–58.
- [6] D. S. Kosov, P. L. A. Popelier, Atomic partitioning of molecular electrostatic potentials, *J. Phys. Chem. A* 104 (2000) 7339–7345.
- [7] K. E. Laidig, R. F. W. Bader, Properties of atoms in molecules. Atomic polarizabilities, *J. Chem. Phys.* 93 (1990) 7213–7224.

- [8] A. Martín Pendás, Stress, virial, and pressure in the theory of atoms in molecules, *J. Chem. Phys.* 117 (2002) 965–979.
- [9] T. A. Keith, R. F. W. Bader, Calculation of magnetic response properties using Atoms in Molecules, *Chem. Phys. Lett.* 194 (1992) 1–8.
- [10] M. A. Blanco, A. Martín Pendás, E. Francisco, Interacting quantum atoms: a correlated energy decomposition scheme based in the quantum theory of atoms in molecules, *J. Chem. Theory Comput.* 1 (2005) 1096–1109.
- [11] E. Francisco, A. Martín Pendás, M. A. Blanco, A molecular energy decomposition scheme for atoms in molecules, *J. Chem. Theory Comput.* 2 (2006) 90–102.
- [12] A. Martín Pendás, A. Costales, V. Luaña, Ions in crystals: the topology of the electron density in ionic materials. I. Fundamentals, *Phys. Rev. B* 55 (1997) 4275–4284.
- [13] T. A. Keith, Computational improvements for the theory of atoms in molecules, Ph.D. thesis, McMaster University (1993).
- [14] F. W. Biegler-König, R. F. W. Bader, T. H. Tang, Calculation of the average properties of atoms in molecules .2., *J. Comput. Chem.* 3 (3) (1982) 317–328.
- [15] F. W. Biegler-König, Calculation of atomic integration data, *J. Comput. Chem.* 21 (12) (2000) 1040–1048.
- [16] P. L. A. Popelier, Integration of atoms in molecules: A critical examination, *Mol. Phys.* 87 (5) (1996) 1169–1187.
- [17] P. L. A. Popelier, A method to integrate an atom in a molecule without explicit representation of the interatomic surface, *Comput. Physics Commun.* 108 (2-3) (1998) 180–190.
- [18] P. L. A. Popelier, A fast algorithm to compute atomic charges based on the topology of the electron density, *Theor. Chem. Acc.* 105 (4-5) (2001) 393–399.
- [19] J. Cioslowski, A. Nanayakkara, M. Challacombe, Rapid evaluation of atomic properties with mixed analytical numerical-integration, *Chem. Phys. Lett.* 203 (2-3) (1993) 137–142.
- [20] J. Cioslowski, An efficient evaluation of atomic properties using a vectorized numerical-integration with dynamic thresholding, *Chem. Phys. Lett.* 194 (1-2) (1992) 73–78.
- [21] M. Rafat, P. L. A. Popelier, Visualization and integration of quantum topological atoms by spatial discretization into finite elements, *J. Comput. Chem.* 28 (2007) 2602–2617.
- [22] V. Luaña, A. Costales, A. Martín Pendás, Ions in crystals: the topology of the electron density in ionic materials. II. The cubic alkali halide perovskites, *Phys. Rev. B* 55 (1997) 4285–4297.

- [23] M. Rafat, M. Devereux, P. L. A. Popelier, Rendering of quantum topological atoms and bonds, *J. Mol. Graph. Model.* 24 (2) (2005) 111–120.
- [24] O. K. Andersen, Linear methods in band theory, *Phys. Rev. B* 12 (1975) 3060–3083.
- [25] G. K. H. Madsen, P. Blaha, K. Schwarz, E. Sjöstedt, L. Nordström, Efficient linearization of the augmented plane-wave method, *Phys. Rev. B* 64 (2001) 195134.
- [26] K. Schwarz, P. Blaha, G. K. H. Madsen, Electronic structure calculations of solids using the wien2k package for material sciences, *Comput. Phys. Commun.* 147 (2002) 71–76.
- [27] K. Schwarz, P. Blaha, Solid state calculations using wien2k, *Comput. Mater. Sci.* 28 (2003) 259–273.
- [28] V. Luaña, L. Pueyo, Simulation of ionic transition-metal crystals: the cluster model and the cluster-lattice interaction in the light of the theory of electronic separability, *Phys. Rev. B* 39 (1989) 11093–11112.
- [29] V. Luaña, L. Pueyo, Simulation of ionic crystals: the *ab initio* perturbed-ion method and application to alkali hydrides and halides, *Phys. Rev. B* 41 (1990) 3800–3814.
- [30] M. A. Blanco, V. Luaña, A. Martín Pendás, Quantum mechanical cluster calculations of ionic materials: Revision 10 of the *ab initio* perturbed ion program, *Comput. Phys. Commun.* 103 (1997) 287–302.
- [31] P. Hohenberg, W. Kohn, Inhomogeneous electron gas, *Phys. Rev. B* 136 (1964) B864–B871.
- [32] W. Kohn, L. J. Sham, Self-consistent equations including exchange and correlation effects, *Phys. Rev.* 140 (1965) A1133–A1138.
- [33] R. McWeeny, *Methods of Molecular Quantum Mechanics*, 2nd Edition, Academic Press, London, 1992.
- [34] S. Huzinaga, A. A. Cantu, Theory of separability of many-electron systems, *J. Chem. Phys.* 55 (1971) 5543.
- [35] S. Huzinaga, D. McWilliams, A. A. Cantu, Projection operators in hartree-fock theory, *Adv. Quantum Chem.* 7 (1973) 187.
- [36] M. A. Blanco, Métodos cuánticos locales para la simulación de materiales iónicos. Fundamentos, algoritmos y aplicaciones, Tesis doctoral, Universidad de Oviedo (1997).
- [37] A. Martín Pendás, M. A. Blanco, A. Costales, P. Mori-Sánchez, V. Luaña, Non-nuclear maxima of the electron density, *Phys. Rev. Lett.* 83 (1999) 1930–1933.
- [38] V. Luaña, P. Mori-Sánchez, A. Costales, M. A. Blanco, A. Martín Pendás, Non-nuclear maxima of the electron density on alkaline metals, *J. Chem. Phys.* 119 (2003) 6341–6350.

- [39] V. Luaña, A. Martín Pendás, J. M. Recio, E. Francisco, M. Bermejo, Quantum mechanical cluster calculations on ionic materials: The *ab initio* perturbed ion (version 7) program, *Comput. Phys. Commun.* 77 (1993) 107–134.
- [40] T. Williams, C. Kelley, Gnuplot. An interactive plotting program, available at <http://www.gnuplot.info>.
- [41] Swiss National Supercomputer Center (CSCS), Molekel: multiplatform molecular visualization program, first versions by P. F. Flükiger and S. Portman. <http://www.cscs.ch/molekel/>.
- [42] V. Luaña, Tessel2 molecular modeller, <http://web.uniovi.es/qcg/tessel>.
- [43] The POV team, Pov-ray: Persistence of vision raytracer, <http://www.povray.org/>.
- [44] A. Martín Pendás, V. Luaña, The curvature of interatomic surfaces. II. Origin and systematics, *J. Chem. Phys.* 119 (2003) 7643–7650.
- [45] D. Goodger, reStructuredText: a lightweight markup language, <http://docutils.sourceforge.net/rst.html>.
- [46] M. Phillips, T. Munzner, S. Levy, Geomview: a 3D interactive geometry program, <http://www.geomview.org>.